CHEMISTRY OF MATERIALS

Article

pubs.acs.org/cm

Molecular Insight into CO_2 "Trapdoor" Adsorption in Zeolite Na-RHO

François-Xavier Coudert[†] and Daniela Kohen*[,†,‡]

[†]Chimie ParisTech, PSL Research University, CNRS, Institut de Recherche de Chimie Paris, 75005 Paris, France

[‡]Department of Chemistry, Carleton College, Northfield, Minnesota 55057, United States

Supporting Information

ABSTRACT: Among other zeolites, sodium-substituted zeolite Na-RHO exhibits a phenomenon known as "trapdoor" adsorption, with extra-framework cations acting as gates to small windows in the zeolite structures. While carbon dioxide can diffuse through these gates, methane and other guests cannot, leading to strong potential for gas separation. This effect has been attributed in the literature to specific cation−guest interactions that would allow CO_2 to pull open the trapdoor. We investigate here the gating phenomenon using *ab initio* molecular dynamics simulations combined with free energy methods. Our findings invalidate this previously proposed mechanism, showing that the presence of CO_2 does not significantly affect the motion of the gating cation. We put forward and demonstrate an alternative mechanism, showing that the amplitude of the thermal motion of the cations is large and that CO_2 is able to squeeze while the gate is open, while nonpolar guests such as methane cannot. This leads to an image of the mechanism that is closer to swinging doors than trapdoors.

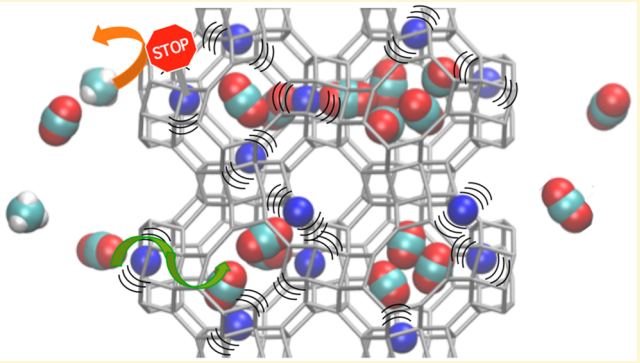

INTRODUCTION

Effective carbon capture processes require materials with a strong ability to discriminate between carbon dioxide and other gases.[1] Microporous adsorbents, such as zeolites and metal−organic framework materials, have received a great deal of attention in a drive to reduce greenhouse gas emissions because of their potential applications in gas separation, capture, and storage. These materials are also being studied given their potential applications in catalysis and other gas separation and storage processes.[2,3]

A particularly promising class of materials for carbon capture are those exhibiting cation gating, a phenomenon that allows carbon dioxide but not other sorbents to permeate them. This is the case for some cationic zeolites whose extra-framework cations block the entrances of narrow pores connecting large cages, allowing cations to act as "trapdoors". Only carbon dioxide can then diffuse through the materials, bypassing the cations and moving from cage to cage. This cation gating gives rise to very high adsorption selectivities for CO_2 over other small adsorbates, which cannot diffuse through the material.

Some members of the zeolite RHO and CHA (chabazite) family exhibit this behavior. Lozinska and co-workers[4−6] demonstrated that zeolite RHO materials with a Si/Al framework ratio around 4 have both good CO_2 uptake and high CO_2 selectivity with respect to small molecules like nitrogen, methane, and ethane. Similarly, chabazite zeolites CsCHA and KCHA exhibit remarkably high selectivity for carbon dioxide over methane.[7−9] However, the molecular mechanism by which carbon dioxide passes through narrow pores blocked to other gases by cations is not well understood at the microscopic scale. Studies based on crystallographic and density functional theory (DFT) evidence highlight the role of carbon dioxide−cation interaction and the collective effects requiring the presence of several CO_2 molecules for the trapdoor to open.[7−9] However, these approaches cannot take into account the dynamical nature of the phenomenon or the realistic CO_2 loading in the unit cell. Molecular dynamics simulations, on the other hand, offer an ideal tool for investigating the mechanism at play.

In this work, we used *ab initio* molecular dynamics (AIMD) to study at the atomistic level the phenomenon of cation gating in the fully exchanged zeolite Na-RHO (3.80 Si/Al ratio). This Na-RHO structure is the most studied of the RHO family of zeolites and the most promising for practical applications because of its selective adsorption properties and low cost. The zeolitic RHO topology[10] (Figure 1) is typical of small pore zeolites with window dimensions close to the kinetic diameter of the relevant gases and cage sizes that facilitate interaction with the adsorbing molecules. It has a three-dimensional channel system composed of one-size cavities (α-cages). Each α-cage is connected to six other α-cages by double eight-ring pores (D8R). This connectivity gives rise to two interpenetrated pore systems, which are not interconnected. Zeolite Na-RHO is known to exhibit some slight flexibility: when the zeolite is loaded with 1 bar of carbon dioxide, the eight rings are distorted, the α-cages become tetrahedral rather than cubic, and

Received: September 9, 2016
Revised: February 27, 2017
Published: February 28, 2017

DOI: 10.1021/acs.chemmater.6b03837
Chem. Mater. 2017, 29, 2724−2730

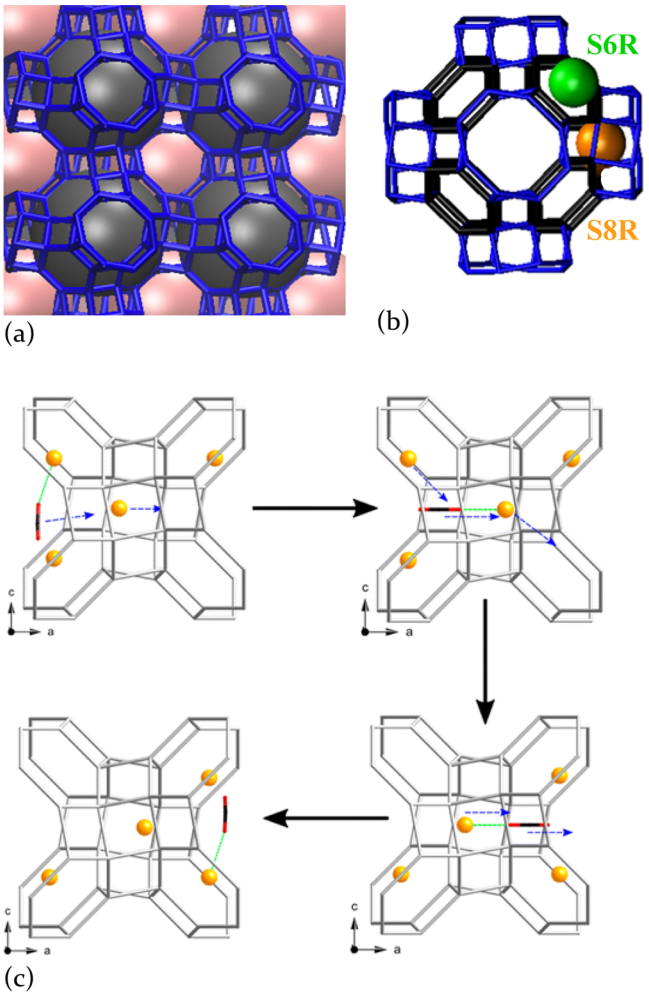

Figure 1. (a) Structure of zeolite Na-RHO upon its exposure to 1 bar of CO_2. The framework is colored blue. Note the three-dimensional channel system composed of cavities (α-cages). Each α-cage is connected to six others by double eight rings (D8Rs). Gray and pink spheres are cages belonging to the two interpenetrated but not interconnected pore systems. (b) Representation of the Na^+ cation sites. Spheres showing preferred cation sites: orange for S8R and green for S6R. The figure also shows the D8R traced in blue and the S6R traced in black. Each unit cell has six D8R sites (and thus 12 S8R sites) and eight S6R sites. The structure shown is that of the empty zeolite. Via comparison of panels a and b, note the slight distortion that occurs upon carbon dioxide adsorption. (c) Mechanism proposed by Lozinska and co-workers[5] at low carbon dioxide coverage. Reproduced with permission from ref 5. Copyright 2012 American Chemical Society. Note how in this mechanism the blocking cation first moves from one S8R site to its partner S8R site and then to a S6R site to allow for the passage of CO_2. The green lines are meant to emphasize the role of the cation−carbon dioxide interaction (which Lozinska et al. presume would have an even larger stabilizing role in the presence of more carbon dioxide molecules).

the zeolite expands approximately 1.5% (but maintains its symmetry in the $I\bar{4}3m$ space group).[5,6] This can be visualized in Figure 1, as well as in three dimensions using the CIF files for both structures that we have included as Supporting Information. Lozinska et al. have determined using X-ray diffraction that Na^+ cations preferentially occupy S8R (single eight-ring) sites and S6R (single six-ring) sites (see Figure 1a), with or without CO_2. The cations that sit in the S8R are the cations that block diffusion within the materials. The Si/Al ratio and site occupancies are such that all narrow pores are likely to blocked.

Previous work on carbon dioxide within this zeolite using classical molecular dynamics, based on an empirical force field and a rigid description of the zeolite framework, suggested that electrostatic interactions between CO_2 and zeolite produce a favorable binding site beyond the gate. This would opportunistically allow CO_2 to partly enter the channel as the cation gate undergoes thermal fluctuations, although no actual crossing of the window was observed.[11] Figure 2 shows a rare event

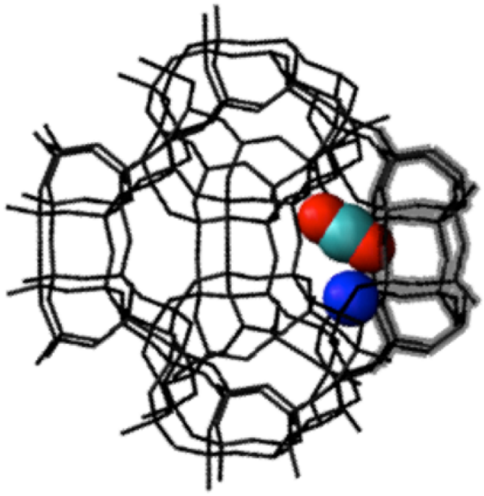

Figure 2. Hint of the microscopic mechanism of gating, observed via classical MD simulations: a carbon dioxide molecule entering a double 8-ring (D8R) blocked by a cation (blue). Only the relevant adsorbate molecule and cation are shown in the figure (there are 9 more cations and 14 more guest molecules in the classical molecular dynamics simulation). The blocked D8R is highlighted.

observed during classical simulation as the carbon dioxide molecule enters a D8R blocked by a cation (blue). Presumably, the fact that other guest molecules lack such strong interaction with the zeolite results in their inability to squeeze by the gating cation. These observations hint at a mechanism that differs from the one suggested earlier (see Figure 1c) in that the crucial interaction is that of carbon dioxide with the zeolite, and thus, the CO_2 does not have an active role on moving the blocking Na^+ out of the way and into a different site.

To gain a good understanding of the mechanism for cation gating at a microscopic level, we need to go beyond the limitations of classical simulations or time-indepent experimental results. Given the inherent difficulty of obtaining experimental mechanistic information at the microscopic scale, we turned to high-accuracy computational condensed matter simulations. Computational advances now make this type of system tractable for *ab initio* molecular dynamics (AIMD), and several studies have highlighted the potential of AIMD to shed light on framework−guest and cation−guest interactions in cationic zeolites.[12−14] Below we present our results using AIMD to further demonstrate carbon dioxide's unique "gate opening behavior" in which its preference for binding inside the "gate" allows CO_2 to "squeeze" by the thermally fluctuating gatekeeping cation.

DOI: 10.1021/acs.chemmater.6b03837
Chem. Mater. 2017, 29, 2724−2730

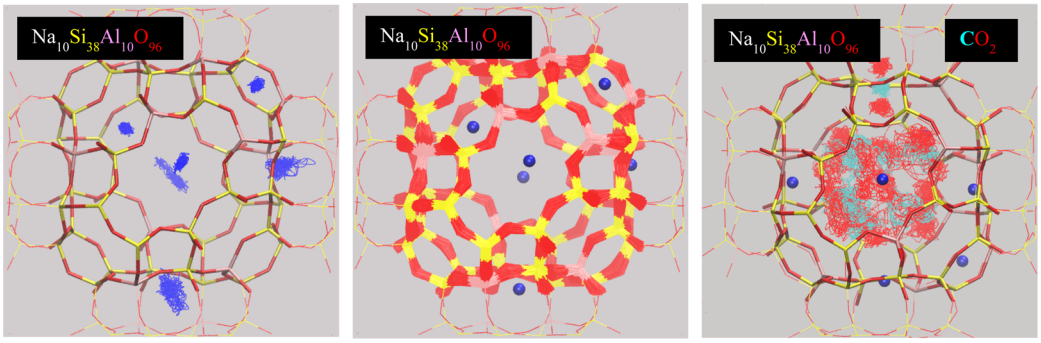

Figure 3. Representative *ab initio* molecular dynamics trajectories. (a) System without guest molecules, with blue traces corresponding to the cation motion. For the sake of clarity, only cations adsorbed on the central cage shown are displayed, and the rest of the zeolite is shown at its average positions. (b) System without guest molecules, with traces corresponding to the motion of framework atoms. The cations are shown at their average positions. (c) Zeolite Na-RHO under 1 atm of carbon dioxide. For the sake of clarity, only molecules adsorbed on the central cage shown are displayed, and the rest of the zeolite is shown at its average positions.

RESULTS AND DISCUSSION

***Ab Initio* Molecular Dynamics.** We first performed unconstrained (free) *ab initio* molecular dynamics simulations of the Na-RHO zeolite, both without any guest molecules and loaded with 15 molecules of CO_2, which corresponds to a pressure of 1 atm of CO_2 (see Computational Methods for details). Figure 3 gives the reader a qualitative idea of the region of space sampled by each atom in the system. Panels a and b of Figure 3 correspond to the same representative trajectory simulating a Na-RHO zeolite without any adsorbate, showing the average positions of all atoms (spheres and cylinders), as well as trajectories of individual species (thin lines denote Na^+ in Figure 3a and framework atoms in Figure 3b). Figure 3c corresponds to another representative trajectory simulating the Na-RHO zeolite loaded with carbon dioxide. We can see while framework atoms vibrate around their equilibrium positions, the sodium cations show a relatively large amplitude of motion (up to 1 Å depending on the particular site) around the S8R and S6R sites, with locations that correspond well to the experimental crystallographic sites presented by Lozinska et al.[6] (see the Supporting Information). Finally, we note that carbon dioxide molecules sit preferentially on the S8R but also explore the cage, also in agreement with experimental evidence.

To provide a quantitative analysis of atomic motion and to look for vibrational modes that could correspond to a concerted motion involving the blocking cation and carbon dioxide, we analyzed the AIMD trajectories using the effective normal mode method.[15] The details of this analysis are shown in the Supporting Information and show that there is no unique vibration mode responsible for the gating phenomenon. Instead, we find that there are ∼120 modes that invoke significant cation motion. With only 10 cations in the system, these modes also have contributions of many other atoms and correspond to heavily delocalized motions (e.g., "window breathing") that are a generic feature of zeolite frameworks.[13]

Given that a CO_2 molecule entering the narrow pore or a cation moving from one site to another is likely to be a rare event, it is not surprising that neither was seen in the unconstrained simulations presented here. The computational demands of AIMD are such that free simulations long enough to witness one are prohibitive. To capture the mechanism, we thus turned to free energy calculations using constrained molecular dynamics and the blue moon ensemble method[16,17] (see Computational Methods for details).

The mechanism governing the passage of carbon dioxide, unlike other gases such as methane, from cage to cage in Na-RHO despite the presence of the blocking cation can be uncovered by evaluating the height of the free energy barriers involved. To circumvent the fact that an unconstrained MD simulation is very unlikely to sample a point high on the barrier, we use constrained *ab initio* molecular dynamics to "force" the system to cross the barrier. Following the blue moon approach, averaging the constraint forces gives a quantitative indication of how stable that particular configuration is, and integrating these forces along the reaction coordinate gives the configuration free energy as a function of constraint coordinate.

Free Energy Profile: Sodium Cation Leaving the Blocking S8R Site. Previous literature about cation gating in Na-RHO suggests[5,6] that the interaction of carbon dioxide with a blocking Na^+ cation allows it to "pull" the cation away briefly from the S8R site and into the S6R site. It is then suggested that during this brief interval CO_2 enters the narrow pore. This scenario can be investigated by evaluating the free energy barrier for a cation to move from the blocking S8R site into the cage and onto a S6R site, in the absence and presence of carbon dioxide. For the suggested scenario to be confirmed, the barrier must be significantly lower in the presence of guest molecules.

We thus compute free energy profiles as a function of the Na^+ cation coordinate perpendicular to a S8R plane, which corresponds to the direction of the cation leaving the S8R. This reaction coordinate, which we denote as $x(\mathrm{COM}-\mathrm{Na}^+)$, corresponds to the projection of the Na^+ cation's position on the x axis (as depicted in Figure 4a) while the cation is allowed to move freely in the $y-z$ plane. For the sake of convenience, its zero is chosen as the center of mass (COM) of the zeolitic framework.

The free energy profiles of the Na^+ cation along this direction, both with and without CO_2, are plotted in Figure 4b. They were obtained by running a series of constrained MD simulations with different values of $x(\mathrm{COM}-\mathrm{Na}^+)$. Apart from the constrained cation, all other atoms in the system were allowed to move freely. $x(\mathrm{COM}-\mathrm{Na}^+)$ ranges from 3.6 to 7.2 Å, where the first value corresponds to a cation that has access to the nearest S6R site (Figure 4a) and the second to the edge of the unit cell (and thus the midpoint between the two S8R sites that make a D8R site).

Figure 4b shows the free energy profiles obtained in the absence and presence of 1 atm of carbon dioxide. It is clear that

DOI: 10.1021/acs.chemmater.6b03837
Chem. Mater. 2017, 29, 2724−2730

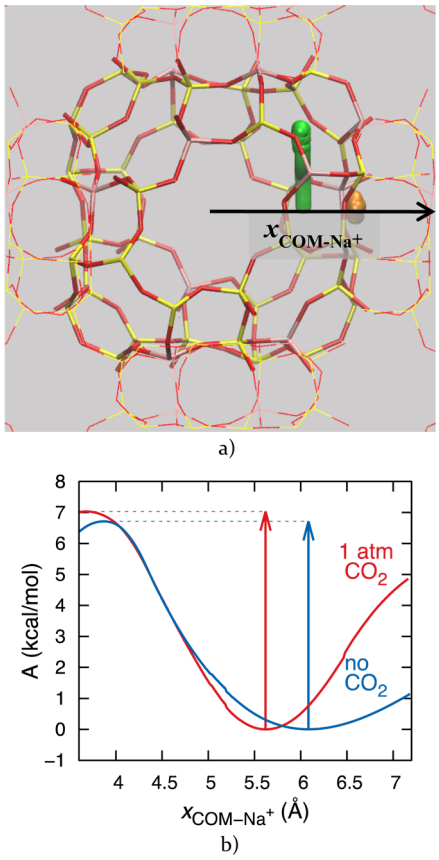

Figure 4. (a) Scheme of the reaction coordinate corresponding to a cation leaving the single 8-ring (S8R). For the sake of convenience, the zero was chosen as the center of mass of the framework. Orange corresponds to the trajectory of a cation constrained to an x(COM−Na^+) of 5.76 Å and green to a cation constrained to an x(COM−Na^+) of 3.6 Å. The trace corresponds to the constrained trajectory (moving only in the y−z plane) in the absence of adsorbed molecules. (b) Free energy profile for a cation leaving the S8R site: blue line for the profile in the absence of carbon dioxide and red line for $P(CO_2)$ = 1 atm.

the free energy barrier is not significantly smaller when there is carbon dioxide present (7.0 kcal/mol vs 6.7 kcal/mol). Thus, the calculated free energy profiles indicate that carbon dioxide molecules do not facilitate the movement of the Na^+ cation out of the S8R site. This contradicts the mechanism proposed in earlier work, based on 0 K DFT calculations of the energy of cation displacement. This highlights the need to account for thermal effects and entropy, which was done in our molecular dynamics simulations and through the use of free energy methods.

The free energy profiles do show, however, that, in the presence of CO_2, Na^+ cations are less likely to migrate to the partner S8R (the ring that makes a D8R with the ring where the cation sits) that we denote S8R*. Moreover, the site they occupy is displaced by 0.5 Å into the cage (from x = 6.1 Å to x = 5.6 Å), and the free energy well becomes more symmetric. Figure 3c points to the reason behind this behavior. Each D8R contains a cation sitting on a S8R and a carbon dioxide sitting on S8R*, with an optimal Na^+−CO_2 distance "pushing" the cation slightly because of their interaction. This is confirmed by visual inspection of the constrained trajectories, highlighting the formation of CO_2/Na^+ pairs in D8R.

It should finally be noted that the validity of these arguments rests on the appropriateness of the coordinate being used for the free energy profiles. When carbon dioxide is present, the "true" reaction coordinate is likely to depend also on the positions of the adsorbed molecules. However, the data presented here indicate that the mechanism is not likely to be that of carbon dioxide molecules interacting with a cation in a way that facilitates opening of the trapdoor. We thus turn to explore another option for the mechanism at play.

Free Energy Profile: CO_2 Molecule Entering the S8R. From the mechanism hint gathered from classical simulations presented in the Introduction (and depicted in Figure 2) and the free energy profile just presented, studying how the free energy profile of a guest molecule entering a S8R from the cage is affected by the presence of a nearby cation appears to be worthwhile. Moreover, we note in Figure 3a that Na^+ has a relatively large amplitude of motion, and from Figure 4b, we see that 2 kcal/mol allows a cation to move from its S8R site into the cage by ∼1 Å. Thus, at 298 K, ∼3% of the time the trapdoor is a little ajar, simply by means of thermal motion. Of course, a similar fraction of the time the cation would be exploring the space further from the cage, moving toward the partner S8R*. In the presence of carbon dioxide, this other ring is likely to be occupied by another carbon dioxide, and thus, it is not likely that such an "exploration" would result in an opening for a passing adsorbate.

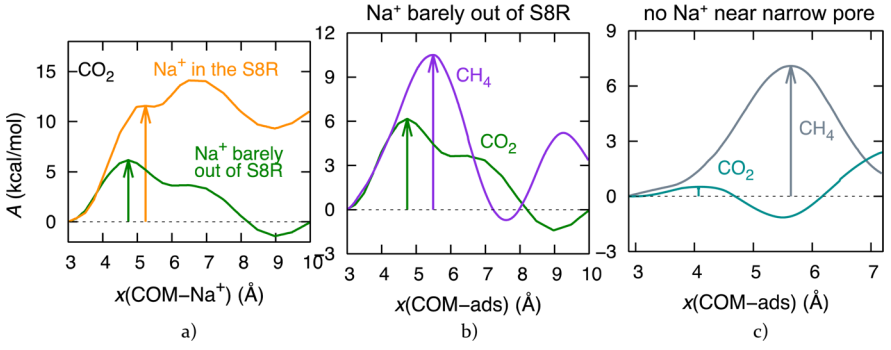

Figure 5. Free energy profile for a guest molecule entering the single 8-ring (S8R). (a) Results for CO_2 obtained when a cation is constrained to x(COM−Na^+) = 5.76 Å (S8R) (orange) and when the cation is constrained to x(COM−Na^+) = 4.68 Å (green). (b) Profile when the cation is constrained to x(COM−Na^+) = 4.68 Å and thus the cation is out of its equilibrium position. Results for carbon dioxide are colored green while those for methane purple. (c) Profiles obtained when all cations can move freely (and none of them was located in a blocking position). Gray shows the results for methane, while aqua shows the results for carbon dioxide.

DOI: 10.1021/acs.chemmater.6b03837
Chem. Mater. 2017, 29, 2724−2730

We thus calculated the free energy profiles for a carbon dioxide molecule entering the narrow pore from the cage, in two different situations: (1) when a cation is sitting in its S8R site, with a constrained coordinate $x(\mathrm{COM-Na^+})$ of 5.76 Å, and (2) when the cation is displaced, with a constrained coordinate $x(\mathrm{COM-Na^+})$ of 4.68 Å. For both situations, the free energy profiles for CO_2 were calculated as a function of the x-axis projection of the COM of the carbon dioxide (with the origin still set at the COM of the zeolitic framework). The free energy profiles for CO_2 are plotted in Figure 5a. Immediately, it is clear that a modest displacement of the sodium cation leads to a significant decrease, by a factor of 2, of the free energy barrier for carbon dioxide to enter the ring (from 11.6 to 6.2 kcal/mol). This decrease and the low value of the resulting free energy barrier are key to explaining the observed diffusion of CO_2 and the gating phenomenon. The large amplitude of the thermal motions of Na^+ out of its crystallographic position allows the carbon dioxide to diffuse through the gate.

The profiles in this case have been extended beyond the limit of the unit cell to allow for the fact that there is no symmetry between the SR8 sites of the two partners. On the cage side, there is a cation sitting on (or near) the ring, while this is not the case on the other side. The minima at ∼9 Å correspond to the stable S8R site for carbon dioxide. The fact that carbon dioxide has a stable site on the S8R is crucial to the understanding of the process. It is only because this is the case that the carbon dioxide is able to squeeze by the cation while the latter is out of its equilibrium position. Figure 5c shows a free energy profile for carbon dioxide obtained when no cation was constrained so that all Na^+ ions were allowed to evolve freely and none was occupying the relevant narrow pore. The profile clearly shows that the S8R is a favorable site for a carbon dioxide.

Moreover, visual inspection and comparison of the geometry of the framework when the CO_2 is outside the S8R or constrained inside reveal that deformation of the framework, in the vicinity of the S8R, is necessary for the guest molecule to pass. The S8R aperture, measured in the narrowest dimension as the center-to-center distance between the two closest oxygen atoms, changes from an average value of 5.27 Å (when the CO_2 is not in the S8R) to 5.57 Å (when the CO_2 is passing through the S8R).

Finally, we tested our explanation of the mechanism by comparing the situation of carbon dioxide with that of methane, which is experimentally known not to permeate the material. We thus calculated the free energy profile for a methane molecule entering the S8R when the gate was partially open, i.e., with a Na^+ cation constrained at $x(\mathrm{COM-Na^+}) = 4.68$ Å. Figure 5b shows that the barrier is significantly higher for methane than for carbon dioxide, in agreement with the experimental results. Furthermore, inspection of Figure 5c, which was obtained when all cations were allowed to move freely and there was no cation in the D8R of interest, reveals that even in the absence of a cation the barrier for methane diffusion is rather large, much larger than that of carbon dioxide. Both findings are explained by the relatively low affinity of methane for the S8R, irrespective of the presence of a cation: methane sits preferably in the cage rather than in the rings, which are favorable for CO_2 only because of electrostatic interactions.

Finally, we note that the diameter of the narrow pore within Na-RHO obtained using geometric criteria is only 1.9 Å. This is smaller than the kinetic diameters of both CO_2 (3.3 Å in the narrowest dimension) and CH_4 (3.8 Å).[18] Clearly, just looking at the size of the molecules and the pores is not a reliable indicator of the dynamical behavior of the system. Not only its size but also its lack of favorable electrostatic interactions with the host material in the single 8-ring accounts for the exclusion of methane. The difference in the size of the adsorbate molecules, however, raises the possibility that size or shape selectivity plays a role.

CONCLUSIONS

We demonstrate here how the interaction of carbon dioxide with the zeolite Na-RHO's single 8-ring (S8R) allows it to enter the narrow pore from the cage as the cation thermally fluctuates in and out of its blocking site. In this microscopic picture of the mechanism for selective CO_2 adsorption, the sodium cations in the rings act as swinging doors agitated by thermal motion, through which the carbon dioxide can squeeze while they are ajar. Methane, lacking the strong adsorbate−zeolite interaction and thus an adsorption site at the gate entrance, experiences a much larger barrier even when the cation is a bit out of the gate. This is the root of the colossal selectivity reported in earlier experimental work.

As there are no experimental data providing direct proof of the diffusion mechanism, we used computational molecular simulation techniques to observe this mechanism. We relied on first-principles molecular dynamics simulations of the fully flexible material combined with free energy methods to obtain free energy profiles as a function of several relevant reaction coordinates, involving the diffusing guest adsorbate and the blocking cation. To avoid the unfeasibly high computational cost of two-dimensional (2D) free energy methods, we calculated cross sections of this 2D free energy surface by combining constrained dynamics and the blue moon ensemble. This allowed us to reveal the microscopic mechanism at play.

This mechanism is schematized in the abstract graphic. To move from one cage to another, a carbon dioxide approaches a narrow pore on the side of a S8R occupied by a cation that has thermally fluctuated a bit out of its site. This carbon dioxide squeezes into the pore via an activated process and then moves onto the partnering S8R*. Afterward, the carbon dioxide can overcame the small barrier that separates the S8R* site from the cage on the right and thus diffuse through the "blocked" D8R.

This systematic study of zeolite Na-RHO underscores the power of *ab initio* molecular dynamics combined with free energy methods to study activated events such as guest diffusion in narrow pores blocked by cations. It can be entirely transferred to other materials, with different zeolitic frameworks, different cations, or different adsorbate molecules. We expect this *ab initio* methodology to open the way to a more accurate description of guest diffusion at the microscopic level. Moreover, the main conclusions reached here on the importance of cation thermal motion and zeolite−carbon dioxide interactions shed new light on previous models of narrow pore diffusion in zeolites. The mechanism observed is not specific to Na^+ or the RHO framework, and we expect that it could be observed for other cationic zeolites with narrow windows such as CHA or LTA. However, the quantitative details of the cation's thermal fluctuation motions, zeolite window size, and cation−CO_2 interactions will in each case depend on window size, cation size, and cation polarizability.

It puts in perspective the importance of the cation−carbon dioxide interactions, on which many theoretical studies focus

DOI: 10.1021/acs.chemmater.6b03837
Chem. Mater. 2017, 29, 2724−2730

but which may not always be a crucial factor limiting diffusion. We have shown that the cation trapdoor is very often a little open, even in the absence of guest molecules. Carbon dioxide molecules are unlikely to facilitate this behavior but are likely to use the opportunity to get into the almost nominally blocked narrow pore, unlike other adsorbates that lack the preference for that narrow location. In the future, we intend to look at previously proposed diffusion mechanisms of polar species in narrow pore zeolites to reanalyze them in light of our new findings. We also note that the molecular dynamics simulations and free energy studies performed in this work deal with the {adsorbent, adsorbate} system at or near thermodynamic equilibrium, whereas in industrial fixed-bed gas separation processes, kinetics might play an additional role in the permeation of small molecules. Molecular simulations on a larger scale, or mesoscopic modeling, would be required to study the influence of kinetics on dynamic separation of gas mixtures.

COMPUTATIONAL METHODS

The *ab initio* molecular dynamics simulations were performed using the CP2K simulation package,[19] which uses density functional theory to calculate atomic forces "on the fly". Its QUICKSTEP module uses the Gaussian and Plane Wave (GPW) method[20] or a Gaussian and Augmented Plane Wave (GAPW) method,[21] where the electronic density is expanded on a basis of plane waves. In the work presented here, the use of the GAPW scheme for the O and Na atoms and the GPW scheme for Si, C, and H atoms resulted in well-converged forces using a 300 Ry cutoff. We use the Perdew−Burke−Ernzerhof (PBE) functional[22] and D3 dispersion correction from Grimme.[23] The core electrons are treated with the Goedecker−Teter−Hutter pseudopotentials.[24] To avoid unphysical charges, the sodium atoms were represented by DZVP MOLOPT SR[25] basis sets while all other atoms were represented by the TZV2P[25] basis set. The nine outer electrons of Na were treated explicitly, but for all other atoms, only their valence electrons were.

The motion of nuclei follows Newton's equation of motion with a time step of 0.5 fs. At each time step, the wave function is optimized with the self-consistent field convergence criterion set to 1.0×10^{-6} a.u. Simulations were performed in the *NVT* ensemble with a CSVR thermostat,[26] with a time constant of 100 fs. All simulations correspond to 298 K, the temperature at which the behavior of carbon dioxide within this material was studied experimentally.

Seven trajectories of at least 25 ps where obtained for an empty Na-RHO and seven others with 15 carbon dioxide molecules (the loading at 1 atm, the pressure at which experimental data are available). In all cases, one unit cell was simulated and periodic boundary conditions were used. The initial positions for the cations and adsorbates used to start AIMD simulations were obtained using classical grand canonical Monte Carlo simulations, while the framework atoms were those determined experimentally. The empty zeolite initial positions and those for the zeolite loaded with guest molecules are those of ref 6. The methods used are described by Bamberger,[11] but note that the interactions between carbon dioxide and the Na-exchanged zeolite were modeled using the CCFF potential[27] recently developed by Sholl and co-workers. This potential necessitates a rigid framework but allows the cations to move. More details about the initial configurations can be found in the Supporting Information.

As mentioned above, free energy profiles were obtained using constrained dynamics and the blue moon ensemble method.[16,17] To compute a free energy profile, at each point along the reaction coordinate, the ensemble average force due to the constraint along the constraint direction was evaluated. When the constraint is a simple distance constraint like the one used in our work, the average force can be related to the change in free energy by $dA/d\zeta^* = -\langle f \rangle_{\zeta^*}$, where f is the force due to the constraint along the constraint direction and ζ^* is the value of the constraint (fixed during a given simulation). The free energy as a function of the reaction coordinate (the free energy profile) is then obtained by integrating the average force along the reaction coordinate.

The constrained *ab initio* molecular dynamics simulations were performed using the CP2K code and the parameters detailed above, with a constant temperature and fixed unit cell parameters. Note that CP2K computes f at each time step, as it is the Lagrange multiplier in the SHAKE algorithm used to constrain the dynamics. To prevent strong oscillations in f, the shake error was required to be $<10^{-8}$ a.u. In all cases, the forces were averaged after evolution for 0.5 ps to capture the system after it had equilibrated. Errors reported correspond to standard deviation errors and were calculated using the block average method with 10 blocks (errors shown in the force graphs in the Supporting Information). A quadratic interpolation scheme was used to integrate the forces and thus to obtain the free energy profiles shown. The center of mass of the guest molecules was used to compute ζ^* to prevent fluctuations related to rotations of the molecules. Care was taken to locate the constraint cation or molecule within the unit cell (avoiding the need to use the periodic boundary conditions in the evaluation of f). The initial configurations were chosen so the cations and guest molecules that were not constrained were relatively well equilibrated with the constrained object. More details are given in the Supporting Information.

ASSOCIATED CONTENT

Supporting Information

The Supporting Information is available free of charge on the ACS Publications website at DOI: 10.1021/acs.chemmater.6b03837.

Cation and carbon dioxide locations, effective normal modes, free energy profiles, and details of the generation of initial configurations for AIMD (PDF)

Crystallographic data for the Na-RHO structure in the absence of carbon dioxide (CIF)

Crystallographic data for the Na-RHO structure under 1 atm of carbon dioxide (CIF)

AUTHOR INFORMATION

Corresponding Author

*E-mail: dkohen@carleton.edu.

ORCID

François-Xavier Coudert: 0000-0001-5318-3910

Daniela Kohen: 0000-0001-7900-1660

Notes

The authors declare no competing financial interest.

ACKNOWLEDGMENTS

We thank Fabien Trousselet, Rodolphe Vuilleumier, Anne Boutin, and Marie-Laure Bocquet for stimulating discussions. We acknowledge access to HPC platforms provided by a GENCI grant (x2016087069) and the National Science Foundation (CHE-1039925) for computing resources.

REFERENCES

(1) Cheung, O.; Hedin, N. Zeolites and related sorbents with narrow pores for CO_2 separation from flue gas. *RSC Adv.* **2014**, *4*, 14480−14494.

(2) Keskin, S.; Sholl, D. S. Efficient Methods for Screening of Metal Organic Framework Membranes for Gas Separations Using Atomically Detailed Models. *Langmuir* **2009**, *25*, 11786−11795.

(3) Yazaydin, A. O.; Snurr, R. Q.; Park, T. H.; Koh, K.; Liu, J.; LeVan, M. D.; Benin, A. I.; Jakubczak, P.; Lanuza, M.; Galloway, D. B.; Low, J. J.; Willis, R. R. Screening of Metal-Organic Frameworks for Carbon Dioxide Capture from Flue Gas Using a Combined Experimental and Modeling Approach. *J. Am. Chem. Soc.* **2009**, *131*, 18198−18199.

DOI: 10.1021/acs.chemmater.6b03837
Chem. Mater. 2017, 29, 2724−2730

(4) Palomino, M.; Corma, A.; Jorda, J. L.; Rey, F.; Valencia, S. Zeolite Rho: a highly selective adsorbent for CO_2/CH_4 separation induced by a structural phase modification. *Chem. Commun.* **2012**, *48*, 215−217.
(5) Lozinska, M. M.; Mangano, E.; Mowat, J. P. S.; Shepherd, A. M.; Howe, R. F.; Thompson, S. P.; Parker, J. E.; Brandani, S.; Wright, P. A. Understanding Carbon Dioxide Adsorption on Univalent Cation Forms of the Flexible Zeolite Rho at Conditions Relevant to Carbon Capture from Flue Gases. *J. Am. Chem. Soc.* **2012**, *134*, 17628−17642.
(6) Lozinska, M. M.; Mowat, J. P. S.; Wright, P. A.; Thompson, S. P.; Jorda, J. L.; Palomino, M.; Valencia, S.; Rey, F. Cation Gating and Relocation during the Highly Selective "Trapdoor" Adsorption of CO_2 on Univalent Cation Forms of Zeolite Rho. *Chem. Mater.* **2014**, *26*, 2052−2061.
(7) De Baerdemaeker, T.; De Vos, D. Gas Separation Trapdoors in Zeolites. *Nat. Chem.* **2013**, *5*, 89−90.
(8) Shang, J.; Li, G.; Singh, R.; Gu, Q. F.; Nairn, K. M.; Bastow, T. J.; Medhekar, N.; Doherty, C. M.; Hill, A. J.; Liu, J. Z.; Webley, P. A. Discriminative Separation of Gases by a "Molecular Trapdoor" Mechanism in Chabazite Zeolites. *J. Am. Chem. Soc.* **2012**, *134*, 19246−19253.
(9) Shang, J.; Li, G.; Singh, R.; Xiao, P.; Liu, J. Z.; Webley, P. A. Determination of Composition Range for "Molecular Trapdoor" Effect in Chabazite Zeolite. *J. Phys. Chem. C* **2013**, *117*, 12841−12847.
(10) Robson, H. E.; Shoemaker, D. P.; Ogilvie, R. A.; Manor, P. C. Synthesis and Crystal-Structure of Zeolite Rho − A New Zeolite Related to Linde Type A. *Adv. Chem. Ser.* **1973**, *121*, 106−115.
(11) Bamberger, N.; Kohen, D. Atomistic Simulations of CO_2 during "Trapdoor" Adsorption onto Na-Rho Zeolite. In *Foundations of Molecular Modeling and Simulation: Select Papers from FOMMS 2015*; Springer: Dordrecht, The Netherlands, 2015; pp 153.
(12) Coudert, F. X.; Vuilleumier, R.; Boutin, A. Dipole moment, hydrogen bonding and IR spectrum of confined water. *ChemPhysChem* **2006**, *7*, 2464−2467.
(13) Coudert, F. X.; Cailliez, F.; Vuilleumier, R.; Fuchs, A. H.; Boutin, A. Water nanodroplets confined in zeolite pores. *Faraday Discuss.* **2009**, *141*, 377−398.
(14) Mace, A.; Laasonen, K.; Laaksonen, A. Free energy barriers for CO_2 and N_2 in zeolite NaKA: an ab initio molecular dynamics approach. *Phys. Chem. Chem. Phys.* **2014**, *16*, 166−172.
(15) Martinez, M.; Gaigeot, M. P.; Borgis, D.; Vuilleumier, R. Extracting effective normal modes from equilibrium dynamics at finite temperature. *J. Chem. Phys.* **2006**, *125*, 144106.
(16) Sprik, M.; Ciccotti, G. Free energy from constrained molecular dynamics. *J. Chem. Phys.* **1998**, *109*, 7737.
(17) Carter, E. A.; Ciccotti, G.; Hynes, J. T.; Kapral, R. Constrained Reaction Coordinate Dynamics for the Simulation of Rare Events. *Chem. Phys. Lett.* **1989**, *156*, 472−477.
(18) Ismail, A. F.; Khulbe, K.; Matsuura, T. *Gas Separation Membranes: Polymeric and Inorganic*; Springer: Dordrecht, The Netherlands, 2015.
(19) http://www.cp2k.org/.
(20) Lippert, G.; Hutter, J.; Parrinello, M. A hybrid Gaussian and plane wave density functional scheme. *Mol. Phys.* **1997**, *92*, 477−488.
(21) Iannuzzi, M.; Hutter, J. Inner-shell spectroscopy by the Gaussian and augmented plane wave method. *Phys. Chem. Chem. Phys.* **2007**, *9*, 1599−1610.
(22) Zhang, Y. K.; Yang, W. T. Comment on "Generalized gradient approximation made simple". *Phys. Rev. Lett.* **1998**, *80*, 890.
(23) Grimme, S.; Antony, J.; Ehrlich, S.; Krieg, H. A consistent and accurate ab initio parametrization of density functional dispersion correction (DFT-D) for the 94 elements H-Pu. *J. Chem. Phys.* **2010**, *132*, 154104.
(24) Goedecker, S.; Teter, M.; Hutter, J. Separable dual-space Gaussian pseudopotentials. *Phys. Rev. B: Condens. Matter Mater. Phys.* **1996**, *54*, 1703−1710.
(25) VandeVondele, J.; Hutter, J. Gaussian basis sets for accurate calculations on molecular systems in gas and condensed phases. *J. Chem. Phys.* **2007**, *127*, 114105.
(26) Bussi, G.; Donadio, D.; Parrinello, M. Canonical sampling through velocity rescaling. *J. Chem. Phys.* **2007**, *126*, 014101.
(27) Fang, H. J.; Kamakoti, P.; Ravikovitch, P. I.; Aronson, M.; Paur, C.; Sholl, D. S. First principles derived, transferable force fields for CO_2 adsorption in Na-exchanged cationic zeolites. *Phys. Chem. Chem. Phys.* **2013**, *15*, 12882−12894.

DOI: 10.1021/acs.chemmater.6b03837
Chem. Mater. 2017, 29, 2724−2730